JOURNAL OF MATERIALS SCIENCE 13 (1978) 155–166

Mössbauer study of Fe-Cr-Co magnetic alloys

M. E. HOUGHTON, P. L. ROSSITER
Department of Materials Engineering, Monash University, Clayton, Victoria, Australia 3168.

P. E. CLARK
Department of Physics, Monash University, Clayton, Victoria, Australia 3168.

Mössbauer spectroscopy has been used to investigate the hyperfine fields in an Fe–27.5% Cr–17.5% Co–0.5% Al alloy for different heat treatments. Spectra for the as-cast condition consist of two superimposed 6 line spectra and a central peak and reveal the three distinct iron environments of α_1, α_2, and γ phases respectively. Following homogenization a broad distribution of hyperfine fields associated with broad isomer shift distribution is indicative of randomized atomic distribution within a single phase. Upon isothermal heat treatment at 620° C the α phase spinodally decomposes into 2 ferromagnetic environments: a Fe–Co rich α_1 phase with $H_{eff} \approx 350$ kOe and a Cr-rich α_2 phase with $H_{eff} \approx 200$ kOe. Evidence of a third ferromagnetic iron rich environment (α_3 phase with $H_{eff} \approx 325$ kOe) is also found as a transition phase which forms prior to subsequent ageing. The progressive reduction in ageing temperature from 600 to 540° C to improve coercivity transforms the α_1 and α_2 modulated structure into a paramagnetic Cr-rich precipitate giving a single line spectrum and a highly ferromagnetic Fe–Co rich matrix giving $H_{eff} \approx 350$ kOe. Anisotropy of the Fe–Co matrix introduced by isothermal decomposition under the influence of the external magnetic field is clearly observable after the ageing process through changes to the Mössbauer spectrum.

1. Introduction

Alloys of iron–cromium–cobalt (~30% Cr, ~20% Co) offer a unique combination of good permanent magnetic properties and machinability [1]. Anisotropic magnet properties similar to those for Alnico 5 are obtainable not only in the form of casting, but also in worked profiles previously only available in lower energy materials such as Cunife, Vicalloy of cobalt-steel. To develop optimum coercivity the alloys are homogenized at ~1250° C quenched to retain a single phase α (b c c) structure and isothermally treated at 600 to 640° C to initiate decomposition into a finely divided two phase (α_1 and α_2) structure. This is followed by a stepped ageing at temperatures reducing from 600° to 540° C. The α_1 and α_2 two-phase structure developed during the initial isothermal decomposition treatment is retained during the stepped ageing process [2]; and this treatment is reported to bring about a change in the composition of the two phases [3]. When very long ageing times are used, i.e. far in excess of those periods necessary to promote optimum coercivity, there is a tendency towards the formation of a σ-phase [3–5]. The neutron diffraction results of Vintaykin *et al.* [6] indicate there is formation of an ordered Fe–Co phase during the isothermal heat treatment (as expected from various thermodynamic arguments [7, 8]) as well as phase segregation, with the second phase presumed to be chromium rich. The simultaneous occurrence of segregation and ordering has been verified by

Ovchinnikov *et al.* [9] using calorimetric and NMR methods. These findings support the original supposition of Kaneko [1] that the hard magnetic properties are derived from the juxtaposition of the finely devided elements of an iron rich phase (α_1), which is strongly ferromagnetic, with a chromium rich (α_2) phase, which is either weakly ferromagnetic or paramagnetic. If a steady directional field ≈ 2 kOe is applied during the isothermal decomposition treatment, anisotropic values of remanence and maximum energy product comparable to some grades of Alnico 5 are obtained in the field direction. This thermomagnetic heat treatment serves to produce a general alignment of the two-phase microstructure but the degree of alignment and its relationship to any particular crystallographic direction remains uncertain. Single crystal measurements by Kaneko *et al.* [10] and Okada *et al.* [11] indicate that the microstructure and direction of magnetic anisotropy are not strongly dependent upon crystal orientation, whereas our own transmission electron microscopy [12] and the studies of Cremer and Pfeiffer [2] indicate a possible preferred alignment in the ⟨1 0 0⟩ directions. Other research concerned with the effect of additional alloying elements [3, 5, 13–22] and cold work [10, 18], has indicated ways in which improvements to magnetic properties may be achieved.

From the various studies which have involved TEM [13], torque magnetometry [23], and X-ray diffraction [3, 24], it would appear that the decomposition of the α phase into the modulated structure [3] is by spinodal mechanism [13] [23, 24] and does not involve nucleation and growth.

Mössbauer spectroscopy provides an alternative and very powerful tool for studying at the atomic level the effects of ageing and field treatments and monitoring the decomposition processes involved (see e.g. [25]). In the only Fe–Cr–Co Mössbauer investigation so far encountered by the present authors, Tahara *et al.* [26] have found that the as-quenched single phase solid solution (α) of an Fe–31% Cr–23% Co alloy is progressively and very rapidly transformed by spinodal decomposition into iron–cobalt and chromium-rich phases. The results for this study have been restricted to the effects of progressive isotropic isothermal decomposition treatments at 560° C using foil specimens thinned after the homogenization stage.

In the sections that follow results are presented for a series of Mössbauer experiments on an Fe–27% Co–0.5% Al alloy subjected to a series of heat treatments. The aim of this study has been to determine the local atomic arrangements which occur when the various metallurgical stages are carried out pursuant to developing optimum permanent magnetic properties. These stages comprise (a) the as-cast condition; (b) following solution treatment; (c) after various isothermal decomposition treatment conditions (initial decomposition processing at different temperatures and for different times, with and without an applied magnetic field); (d) after the subsequent stepped ageing (progressive reduction in temperature from 600° C to 540° C over a period of 13 h) – details of the respective heat treatments are set out in Table II. The chromium and cobalt compositions were chosen to avoid the presence of an σ-phase [18] and the aluminium addition was made to limit the formation of any non-magnetic γ (f c c) phase inclusions [17].

2. Experimental

The alloys were prepared from electrolytic flake iron (99.95% Fe, 0.04% O_2, 0.005% C), electrolytic flake chromium (99.9% Cr), and pure aluminium strip (99.9+% Al). Melting took place in a vacuum induction furnace under a small positive pressure of argon to limit volatilization. Details of

TABLE I Summary of Fe–Cr–Co Ingot Compositions, as-weighed (i.e. as-charged into furnace) and as determined by consultant analyst.

Element	Melt 1		Melt 2	
	As-Charged %	Analysed %	As-Charged %	Analysed %
Cr	27.5	27.8	27.5	27.4
Co	17.5	17.0	17.5	17.4
Al	1.0	0.5	1.2	0.67
C	Impurity presence only	0.06	Impurity presence only	0.04
Fe	bal	bal	bal	bal

the as-charged and final composition (as determined by Spectrometer Services Pty. Ltd.) are shown in Table I. Rod specimens 0.48 mm diameter x 15.9 mm length were machined from the as-cast ingot for subsequent heat treatments, carried out in a globar furnace (with argon atmosphere) for homogenization, and then in a small electric furnace (with air atmosphere) constructed within the pole gap of a 60 mm electromagnet for the isothermal decomposition and ageing treatments. Demagnetization and energy product curves were determined for the rods at each stage of the heat treatment using an integration magnetometer and 100 mm electromagnet. A summary of the heat treatments employed and measured magnetic properties is given in Table II. The rods were then parted-off to a thickness of 0.5 mm using a tool-post grinder and thinned by standard metallographic polishing techniques to disc of 0.042 to 0.048 mm thickness for the Mössbauer study.

Mössbauer spectra were obtained using a constant acceleration electromagnetic transducer drive system to control the motion of a 5 mCi Mössbauer source of either ^{57}Co in Rh or ^{57}Co in Cu. These sources had FWHM against the inner lines of a thin natural iron absorber of 0.32 and 0.27 mm sec^{-1} respectively. All spectra were obtained in transmission geometry with the source and specimen absorber at room temperature and the velocity scale was calibrated before each experiment using a natural α-Fe foil.

For accurate quantitative analysis from Mössbauer spectral areas the effects of absorber thickness must be taken into account. When the effective absorber thickness [25] $t_A \leqslant 1$, the Mössbauer lines can be filled by Lorentzian curves. When $t_A > 1$, the Mössbauer lines are broadened by saturation effects, and the fitting of the hyperfine pattern by a set of Lorentzian curves is no longer possible. For the system under consideration, in order that the condition $t_A < 1$ is fulfilled, it is required that the physical specimen thickness should be $\leqslant 0.025$ mm. However, during specimen preparation when the thickness was reduced to below ≈ 0.04 mm, there occurred a marked tendency towards fragmentation by intergranular fracture. This condition was particularly noticeable for specimens in the initially decomposed and subsequently aged conditions.* As the study demanded the use of undamaged specimens, including some in which field treatment directionality was identifiable, it was decided to use specimens for which t_A was greater than optimum. While it is possible to calculate the transmission integral to allow for the effect of finite absorber thickness, or to use an iterative method of correction [27], the asymmetric distributions of hyperfine fields observed in most of the present samples would further complicate these calculations. Since absolute line widths and line areas were not essential parameters to interpretation of the observed results these calculations were therefore omitted. In computer fitting of the experimental data as a series of six-line and single-line Lorentzian spectra, emphasis was placed on correctly assigning the observed peaks to the appropriate subspectra and on obtaining values for the hyperfine field and isomer shift corresponding to the positions of maximum line intensity.

3. Results

The Mössbauer spectra obtained in the investigation are set out in Figs. 1 to 4. The data obtained from the analyses of these spectra are summarized in Table III. The results obtained at the various stages of heat treatment are considered in more detail below.

3.1. As-cast condition

The Mössbauer spectrum for the as-cast specimen is shown in Fig. 1a and indicates the presence of three distinctly different iron environments. The central peak corresponds to a paramagnetic γ-region having an isomer shift of $-0.11 \pm .02$ mm sec^{-1} with respect to pure α-Fe. The rest of the spectrum corresponds to a superposition of two six-line spectra, that which is more intense having a slightly larger hyperfine splitting. The spectrum with the larger splitting has a hyperfine field of 358 ± 2 kOe and is evidently due to Fe in a Co-rich environment. Because of the peaked nature of the dependence of hyperfine field on Co composition, this measured hyperfine field could indicate a Co content of either $15 \pm 3\%$ or $38 \pm 2\%$ [28]. The second six-line spectrum corresponds to a hyperfine field of 314 ± 6 kOe and is apparently due to Fe in a Cr enriched, though still ferromagnetic,

*It is interesting to note that while preparing the thin specimens, no tendency to fracture in as-cast discs was observed; this is surprising since as-cast brittleness has been reported for Fe–Cr–Co alloys containing Al and Nb [15].

TABLE II Summary of parameters of Fe–Cr–Co Alloy specimens including melt number, heat treatment condition and metallographic (optical and TEM) observations.

Specimen	Melt	See Figure	Heat treatment condition of specimen [see* and † below]	Metallographic structure observed by optical microscopy and TEM	Demagnetization and Energy Product Curve Results					
					Br (kG) ± 0.1	BH_{max} (MG Oe)	bH_c (Oe)	iH_c (Oe)	Bs (kG) ± 0.1	Anisotropy $Br_{\parallel}/Br_{\perp}$
1	2	1a	as cast	Grains of $\alpha_1 + \alpha_2$ decomposition phases and γ plates at GBs and γ plates and	2.7	0.02 ±0.005	30 ±2	32 ±2	12.9	–
2	2	1b	Solution treated for 2 h at 1250° C in argon, water quenched	Virtually single phase α (decomposition not observed). Some traces of γ at grain boundaries and at some regions within the α grains	1.1	0.003 ±0.001	10 ±2	12 ±2	13.5	–
3	2	1c	Solution treated for 2 h at 1250° C in argon, water quenched		0.9	0.003 ±0.001	10 ±2	12 ±2	13.2	–
4	2	1d	Isothermal decomposition treatment of 2 h at 620° C without a field	Grains of $\alpha_1 + \alpha_2$ decomposition phases with some traces of γ in grain boundaries a γ-free zone around the GBs. and in grains remote from the GBs. Higher % of γ observed in No. 4 only. No. 6 and No. 7 show some evidence of field influence on direction of decomposition phases.	3.6	0.03 ±0.005	34 ±2	36 ±2	13.2	–
5	1	1e	Isothermal decomposition treatment of 4 h at 620° C without a field		3.5	0.03 ±0.005	28 ±2	30 ±2	13.3	–
6	1	1f	Isothermal decomposition treatment of 4 h at 620° C in $_{\parallel}$ field of 1 kOe		7.1	0.05 ±0.005	26 ±2	28 ±2	13.2	$Br_{\parallel}/Br_{\perp} = 1.8$
7	1	1g	Isothermal decomposition treatment of 4 h at 620° C in ⊥ field of 1 kOe		3.9	0.05 ±0.005	48 ±2	51 ±2	13.4	

8	1	2a	Isothermal decomposion treatment of 4 h at 600° C without a field and stepped ageing	Grains of $\alpha_1 + \alpha_2$ decomposition product with presence of residual γ phase in small quantities or traces throughout the grains and at the grain boundaries in all examined specimens. No. 13 and No. 14 show some evidence of field influence on direction of decomposition phases.	5.0	0.16 ±0.01	84 ±3	86 ±3	14.1	
9	2	2b 3b 4c	Isothermal decomposition treatment of 4 h at 620e C without a field and stepped ageing		8.1	1.22 ±0.05	442 ±5	445 ±5	13.7	–
10	2	2c	Isothermal decomposition treatment of 4 h at 660° C without a field and stepped ageing		4.2	0.09 ±0.01	54 ±2	56 ±2	14.2	–
11	2	3a	Isothermal decomposition treatment of 30 min at 620° C without a field and stepped ageing.		5.2	0.14 ±0.01	84 ±3	86 ±3	14.1	–
12	2	3c	Isothermal decomposition treatment of 8 h at 620° C without a field and stepped ageing		8.5	0.86 ±0.05	283 ±5	285 ±5	14.0	–
13	2	4a	Isothermal decomposition treatment of 4 h at 620° C in $\parallel$ field of 1 kOe and stepped ageing		12.7	1.25 ±0.05	178 ±4	180 ±4	14.1	$Br_{\parallel}/Br_{\perp} = 1.9$
14	2	4b	Isothermal decomposition treatment of 4 h at 620° C in $\perp$ field of 1 kOe and stepped ageing		6.7	0.44 ±0.02	207 ±4	209 ±4	13.8	

*Samples 4 to 14 inclusive received preliminary solution treatment of 2 h at 1250° C in argon and water quenched, prior to treatments specified.
†Stepped ageing for samples 8 to 14 inclusive comprised a sequence of 1 h each at 600, 580, 570, 560, and 550° C respectively, then 8 h at 540° C.

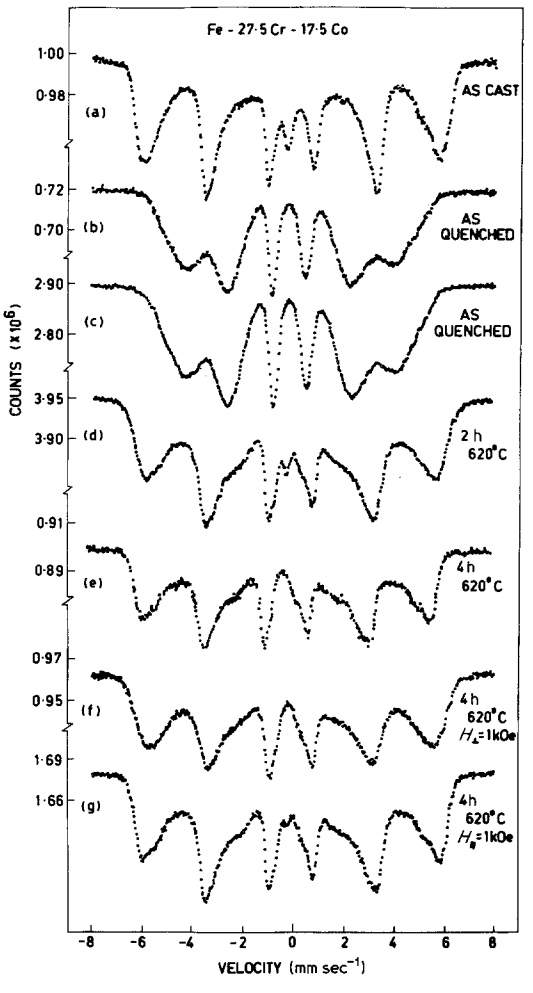

Figure 1 Mössbauer spectra obtained at room temperature for the alloy Fe–27.5 Co in the as-cast and as-quenched conditions, and subsequent to initial decomposition at 620° C. The velocity axis is referred to α-Fe. See text for direction of $H_\perp$ and $H_\parallel$.

environment. This interpretation is supported by the smaller positive isomer shift displayed by this spectrum compared to the Co-rich spectrum. The presence of the γ(f c c) phase and a finely divided $\alpha_1 + \alpha_2$ structure throughout the predominantly remaining b c c regions was verified by optical and electron microscopy [12].

3.2. Quenched from 1250° C

Two specimens of slightly different B_{sat} but similar H_c were examined and gave comparable Mössbauer spectra, as shown in Figs. 1b and c. These spectra are similar to the spectrum of a quenched Fe–31% Cr–23% alloy obtained by Tahara *et al.* [26] and display a broad distribution of hyperfine fields, centred on a value of about 250 ± 6 kOe. Associated with this distribution of fields is a distribution of isomer shifts, evidenced by the substantially dissimilar intensities of the inner pair of lines in the six-lines Mössbauer spectrum, with a mean value of 0.00 ± .05 mm sec^{-1} with respect to α-Fe. This small value reflects the minor change in average s-electron concentration from that of α-Fe expected for alloys in this composition region. The low value of hyperfine field and small isomer shift both indicate a randomized atomic distribution within a single phase structure. Electron microscopy of these specimens also revealed a single phase α (b c c) structure, although small traces of the γ(f c c) phase were occasionally observed. While the incomplete elimination of the γ-phase from these and subsequent specimens was apparent from the electron microscopy, the amount of γ-phase retained was generally so small as to have a negligible effect in the demagnetization curves and to be unobservable in the Mössbauer spectra: The one notable exception was the specimen given an isothermal decomposition treatment of 2 h at 620° C without a magnetic field (see section 3.3 below).

3.3. Initial decomposition treatment

Figs. 1d to g show the spectra obtained from specimens initially decomposed isothermally for 2 and 4 h at 620° C. The spectrum obtained from the specimen for 2 h reveals a central paramagnetic line in addition to two six-line spectra corresponding to two distinct values of hyperfine field. This line has an isomer shift of −0.13 ± .02 mm sec^{-1} and accounts for about 1% of the total spectrum area. A similar, but smaller, line is observed with an isomer shift of −0.14 ± .02 mm sec^{-1} for the specimen held for 4 h in a perpendicularly applied magnetic field of 1 kOe but no such line is apparent for the other specimens held at 620° C for 2 or 4 h. Since pure γ-Fe is known to have a negative isomer shift (−0.07 ± 0.02 mm sec^{-1} with respect to α-Fe) [29], the central paramagnetic line here is attributed to γ-phase contamination, rather than nucleation and growth of a paramagnetic phase. The argument for γ contamination is supported by the larger amount of γ-phase present in the 2 h decomposition specimen compared to the 4 h decomposition specimen as observed by optical and electron microscopy.

The spectra in Figs. 1d to f display evidence for at least two distinct hyperfine fields, with the outer lines (no. 1 and 6) of one field being superposed on the middle lines (nos. 2 and 5) of the other, larger field. In Figs. 1e and g there is also some evidence to suggest presence of an unresolved field intermediate in value between the other, larger field. In Figs. 1e and g there is also resolved fields have values in the region of 350 kOe and 200 kOe. The value of 350 kOe is not substantially different to the 358 kOe observed in the as-cast specimen, and is again interpreted as due to Fe atoms in an Fe–Co environment. On the other hand, the value of about 200 kOe is considerably less than the 314 kOe observed in the as-cast specimen, and, on the assumption that there is no Co in this phase, is due to Fe atoms in an equiatomic Fe–Cr environment [28]. The internal consistency of this assignment is shown by a consideration of the specimen held for 2 h at 620° C. The Mössbauer spectral areas indicate equal numbers of Fe atoms in the two ferromagnetic phases. Thus the Cr-rich phase, assumed equatomic, accounts for 27.5 at.% of the Fe, leaving 27.5 at.% to be combined with the 17.5 at.% Co. The Fe–Co phase would therefore have a composition of ~39 at.% Co, which has a corresponding hyperfine magnetic field of about 358 kOe, the precise value being difficult to determine from the literature as conflicting results have been reported for ordered and disordered specimens [30]. However this value agrees well with the value of 354 ± 3 kOe observed for the Fe–Co phase in this alloy.

A slight reduction in the hyperfine field of the Fe–Cr phase is observed on increasing the time at 620° C from 2 h to 4 h, and, as previously noted, there is some evidence for the appearance of a third ferromagnetic Fe environment having a hyperfine field of about 328 kOe. This value closely corresponds to the 330 kOe observed in pure α-Fe and suggests that some of the Fe is migrating from the Fe–Cr phase to form an iron-rich phase. The interpretation of the spectra for the samples heat treated in a externally applied field of 1 kOe is complicated by the different contributions from the lines 2 and 5 of each spectrum in the two cases. Thus the lines at $+3.5\,\mathrm{mm\,sec^{-1}}$ and $-3.8\,\mathrm{mm\,sec^{-1}}$ in Figs. 1f and 1g are predominantly the outer lines of 200 kOe spectrum in the first case and the middle lines of a 360 kOe spectrum in the second. A unique determination of the degree of polarization of the two Mössbauer spectra is therefore not possible, although it is clear from the increased intensity of lines 2 and 5 in Fig. 1g that the perpendicular field has caused the magnetization of the Mössbauer foil specimen to lie preferentially in the plane of the foil.

The thermomagnetic treatment has also resulted in a degree of anisotropy in the bulk magnetic properties as indicated in Table II

$$(Br_{\parallel}/Br_{\perp} = 1.8).$$

Note that the label ⊥ for the applied field means that the field was applied transversely to the bulk rod sample. Since Mössbauer foils were cut as slices from the rods, a ⊥ applied field here means the field was applied in the plane of the foil sample.

3.4. Stepped ageing treatment

Specimens which had previously received an isothermal decompostion treatment in a manner similar to those described in the previous section, were subjected to an additional stepped ageing treatment in which the temperature was progressively reduced from 600° to 540° C over a period of 13 h, after which time the specimens were water quenched. Additional specimens were also subjected to isothermal decomposition treatments involving a range of times and temperatures, and these also received a stepped ageing treatment similar to the above mentioned specimens. (For details of the decomposition and ageing treatments see Table II). The Mössbauer spectra obtained from the respective sets of specimens are shown in Figs. 2, 3, and 4.

All the spectra for aged specimens show evidence for the presence of two distinct phases, one ferromagnetic and one paramagnetic. The paramagnetic phase which accounts for about 6 ± 0.5% of the total Fe in the specimens, has an isomer shift of $-0.12 \pm 0.02\,\mathrm{mm\,sec^{-1}}$. Very dilute Fe in Cr has an isomer shift of $-0.154 \pm 0.009\,\mathrm{mm\,sec^{-1}}$ [31] and so the single line in the Mössbauer spectra is here interpreted as arising from Cr-rich regions with a low Fe concentration. If all the Cr is contained in this paramagnetic phase then the Fe concentration is ~11.5 at%. Alloys of this composition are known to be paramagnetic at room temperature [32]. Electron microscopy supports this view, since the microstructure is similar to that

TABLE III Summary of Mössbauer parameters for Fe–Cr–Co alloy disc specimens

Specimen	For plot of spectra see Figure	Parameters observed from Mössbauer spectroscopy						
		Phase presence	Magnetic coupling	Hyperfine field H_{eff} (kOe)	Isomer shift (mm sec^{-1}) ±0.02	full width at half maximum (mm sec^{-1})	Fractional area	Comment
1	1a	α_1	ferro	358 ± 2	+0.04	0.81	0.72	
		α_2	ferro	314 ± 6	+0.01	0.87	0.25	
		γ	para		−0.11	0.36	0.03	
2	1b	α	ferro	258 ± 6	0.00	1.25	1.00	
3	1c	α	ferro	264 ± 6	0.00	1.25	1.00	
4	1d	α_1	ferro	354 ± 3	+0.03	1.00	0.43	
		α_2	ferro	203 ± 2	+0.02	0.68	0.56	
		γ†	para		−0.13	0.24	0.01	
5	1e	α_1	ferro	351 ± 2	+0.03	0.72	not detected	
		α_2	ferro	190 ± 4	−0.07	0.75	not detected	
		α_3‡	ferro	322 ± 4	−0.14	0.81	not detected	
6	1f	α_1	ferro	349 ± 3	+0.05	1.24	0.74	
		α_2	ferro	194 ± 2	−0.03	1.27	0.26	
7	1g	α_1	ferro	363 ± 2	+0.05	0.68	0.30	
		α_2	ferro	196 ± 3	−0.09	0.56	0.54	
		α_3‡	ferro	328 ± 4	−0.08	0.93	0.16	
		γ†	para		−0.14	0.38	0.009	
8	2a	α_1	ferro	334 ± 2	+0.04	1.28	0.94	
		α_2	para		−0.11	0.40	0.065	
9	2b 3b	α_1	ferro	348 ± 3	+0.05	0.68	0.94	
	and 4c	α_2	para		−0.11	0.36	0.063	
10	2c	α_1	ferro	354 ± 4	+0.04	0.72	0.94	
		α_2	para		−0.13	0.34	0.060	
11	3a	α_1	ferro	359 ± 2	+0.04	0.84	0.94	
		α_2	para		−0.12	0.44	0.065	
12	3c	α_1	ferro	341 ± 3	+0.04	1.07	0.93	
		α_2	para		−0.11	0.44	0.069	
13	4a	α_1	ferro	347 ± 3	+0.04	1.10	0.94	$X = 0.94$
		α_2	para		−0.11	0.40	0.059	
14	4b	α_1	ferro	351 ± 3	+0.04	0.71	0.94	$X = 2.1$
		α_2	para		−0.11	0.37	0.058	

*Widths for outer lines of hyperfine field spectra
†Presence of γ phase represents ineffective solution heat treatment.
‡Note presence of additional α_3 phase.

observed after the initial isothermal decomposition treatment and no significant γ-phase content is observed in any of these specimens.

The ferromagnetic phase, having a positive isomer shift of $+0.04 \pm 0.01$ mm sec^{-1}, is clearly an Fe–Co rich phase. All the spectra show somewhat broad and asymmetric Mössbauer lines for this phase, indicating slight variations in local atomic distribution. The linewidths quoted in Table III are those corresponding to the high velocity half of the outer lines for each spectrum, and give some measure of the distribution of hyperfine fields quoted in Table III are those corresponding to the most probable values within the distributions. The effects of specific variations in the initial isothermal decomposition treatment prior to the stepped ageing are now considered separately.

3.4.1. *Effect of variation of initial isothermal decomposition temperature*

The Mössbauer spectra for the specimens isothermally processed in zero field for 4 h at temperatures of 600, 620 and 660° C and subsequently aged are shown in Fig. 2. The spectra show an increase in hyperfine field from 334 ± 2 kOe at 600° C, through 348 ± 3 kOe at 620° C to 354 ± 4 kOe at 660° C, with a substantial reduction in the linewidth on going from 600 to 620° C. The bulk magnetic properties also reveal maximum values of remanence and

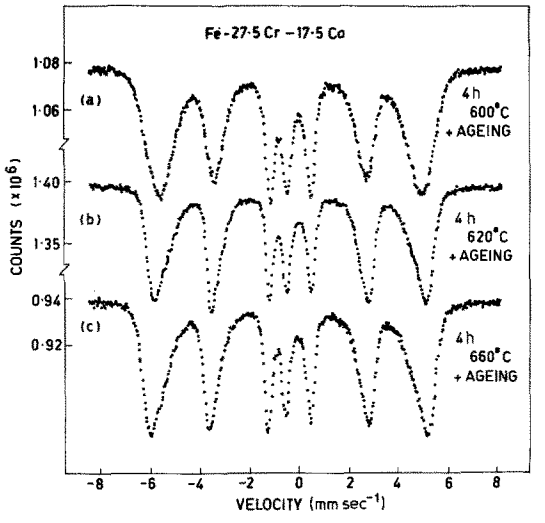

Figure 2 Mössbauer spectra indicating the effect of variation of initial decomposition temperature on the alloy Fe–27.5 Cr–17.5 Co.

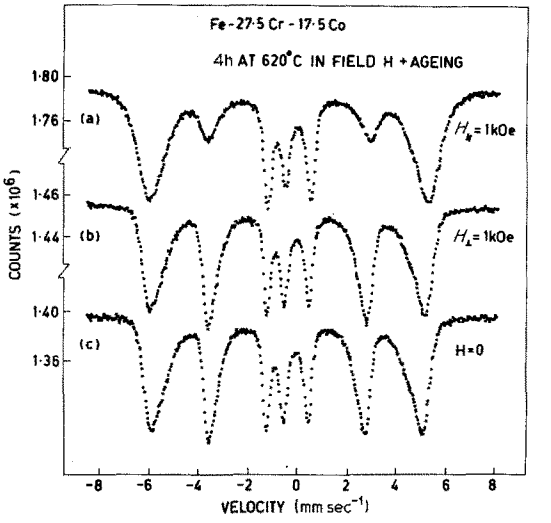

Figure 3 Mössbauer spectra obtained for Fe–27.5 Cr–17.5 Co initially decomposed at 620° C for various times.

coercivity at an initial decomposition temperature of 620° C. It is not clear whether the increase in hyperfine field represents a change in composition of the phase or some form of atomic ordering, but it is significant that no change in the intensity or isomer shift of the Cr-rich phase is observed during this process.

3.4.2. Effects of variation of time of initial isothermal decomposition at 620° C

The spectra obtained from the specimens isothermally decomposed for different times at 620° C and subsequently aged are shown in Fig. 3. The hyperfine field reduces with increased decomposition times but again no change is observed in the paramagnetic phase. The specimen which exhibited maximum coercivity (4 h at 620° C and aged, Fig. 3b) also gave minimum half-width of the outer lines of the hyperfine field. However, whether this variation is related to some optimum size of the decomposition phases or simply reflects a random fluctuation in the atomic distribution is uncertain.

3.4.3. Effects of application of a field during initial isothermal decomposition treatment

Specimens cut from the bulk cylindrical samples processed in an external field of 1.0 kOe applied parallel and perpendicular to the cylinder axis and subsequently aged produced the Mössbauer spectra shown in Figs. 4a and b respectively. For comparison, Fig. 4c shows the spectrum for specimen given identical thermal treatment in the absence of an applied field.

In a thin Mössbauer specimen in which the magnetization is randomly distributed, the six lines of a hyperfine field spectrum have areas in the ratio $3:X:1:1:X:3$, with $X = 2$. Anisotropy in the magnetization is revealed by a change in the value of X. $X = 0$ corresponds to a foil specimen in which the magnetization is fully saturated in

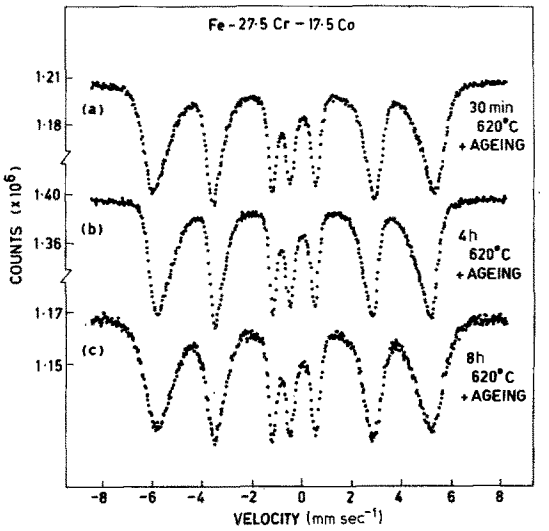

Figure 4 Mössbauer spectra for Fe–27.5 Cr–17.5 Co initially decomposed for 4 h at 620° C in magnetic fields of zero and 1 kOe. Anisotropy of the magnetization is indicated in spectrum (a) by the reduced intensity of the Mössbauer lines at about −3.5 and +3.0 mm sec^{-1}.

the direction of propagation of the Mössbauer γ-rays, and for a conventional system this is normal to the plane of the foil. $X = 4$ corresponds to a specimen in which the magnetization lies wholly in the plane of the foil. The spectrum in Fig. 4a has a value of $X = 0.94$, which indicates the presence of considerable induced anisotropy. If the magnetization had a unique direction, this would be at an angle of 38° to the normal to the foil. What is more likely in a thin foil specimen of this type is that the magnetization within the foil lies along an easy direction nearly parallel to the normal to the foil, while the surface magnetization lies in the plane of the foil.

No substantial anisotropy, ($X = 2.1$) is observed in the specimens in which the field was applied perpendicular to the cylinder axis. This smaller change may be expected, since the larger demagnetizing factor across a long cylinder compared to along its length reduces the effective field during the thermomagnetic treatment.

4. Discussion

The absence of a paramagnetic line in the spectra for the specimens decomposed up to 4 h at 620° C (with the exception as already noted in 3.3 above), supports the conclusion of Tahara *et al.* [26] that the initial decomposition in these alloys occurs by a spinodal mechanism. However, while these workers noted a continuous atomic rearrangement from the single phase solid solution into the Fe–Co rich ferromagnetic and Cr-rich paramagnetic states, they did not record the presence of the intermediate second ferromagnetic state for the Cr-rich regions noted in the previous section (although critical examination of their results namely, spectra representing the 10 and 200 min decomposition times at 560° C does suggest the development of a second weaker hyperfine field). At the higher initial decomposition temperatures used in the present study, and which are required for the development of optimum magnetic properties (620° C compared to 560° C), the presence of such a ferromagnetic state prior to the formation of the paramagnetic phase is quite clear (see e.g. Fig. 1). Cremer and Pfeiffer [2] have postulated the decomposition of the weakly ferromagnetic Cr-rich phase into an additional and even weaker magnetic phase but could not substantiate this from their electron microscope studies. An analogous transition has been proposed to occur in Alnico type alloys [33–36]. For example, Povolotskiy *et al.* [36] have shown that during the isothermal magnetic anneal the original b c c solid solution (denoted in their paper as β_2) decomposes into a rod-like strongly ferromagnetic precipitate (β) in a weakly ferromagnetic matrix β_2'. On cooling a third more weakly ferromagnetic (or paramagnetic) phase forms (β_2'') from the β_2' and the amount of β increase so that the rod-like regions begin to link up into a cellular structure. During the subsequent ageing the remaining β_2' transforms completely into $\beta + \beta_2''$, the β_2'' now appearing as weakly magnetic rods in a strongly ferromagnetic β matrix. In parallel with these transformations are concentration changes in which the β phase is further enriched by ferromagnetic components at the expense of the weakly magnetic phases. From the evidence of the incompletely resolved spectra for the 3rd ferromagnetic phase which has been designated α_3 (see Table III, specimens 5 and 7), we now propose that a comparable behavioural sequence is also applicable for the decomposition of the Fe–Cr–Co alloys which we have studied. Not only is the existence of an additional weakly ferromagnetic phase clearly evident in the spectra obtained for specimens in the condition subsequent to the initial isothermal decomposition stage, but also its transformation into a paramagnetic phase is confirmed after the stepped ageing. That the strongly ferromagnetic Fe–Co phase is positioned as the interconnected matrix and not in the form of the isolated included regions, is supported by reference to the electrochemical behaviour of the material. During the preparation of thin foils for the electron microscope investigation [12], it was observed that preferential etching of the included phase regions occurred when electrolysing at 30 V in a highly acid (pH ≈ 1) solution of 10% perchloric acid + 90% acetic acid. Electrochemical behaviour such as this would be expected for a chromium rich precipitate in an Fe–Co rich matrix. At the very low level of pH, and under the application of the electrolysing potential the corrosion conditions for all elements are energetically very favourable. However, the lower electrode potentials for chromium, than for either iron or cobalt [37], will promote preferential corrosion of the Cr-rich region particularly as the passivation protection afforded to Cr through the formation of an oxide film is not possible under the highly acid-potential

conditions prevailing [38]. Confirmation of the identification of phase regions is obtained when the theoretically anticipated volume fractions for each phase are considered; for the Fe–Co phase to occupy a volume exceeding that of the Cr-rich phase to the degree indicated by the Mössbauer spectra, would require the ferromagnetic regions to be the matrix, and the paramagnetic regions to comprise the precipitates.

The increase in the hyperfine field exhibited by the Fe–Co rich phase when the initial isothermal decomposition temperature is increased, may be attributable to a larger percentage of Co and/or a change in the state of order in that phase. Either of these factors could have influenced the observed associated change in the bulk magnetic properties; trends in these properties are in broad agreement with those reported by Cremer and Pfeiffer [2]. For example, decomposition temperatures should predictably result in a larger predominent spinodal wavelength (and hence α_2 "particle" size), and in broader composition fluctuations [39]. The dimensions of the strongly ferromagnetic matrix α_1 should also increase with temperature and pass through optimum volume sizes at which the coercivity and remanence are maximized. For the H_c to be at a maximum requires that the volume fraction for the strongly magnetic phase is at the critical domain size, while this does not necessarily conform to the optimum volume size which maximizes *Br*. However, from the demagnetization and energy product results obtained from isotropic specimens the optimum decomposition temperature for both these parameters is in the vicinity of 620° C. Because of the associated changes in the magnitude of the composition fluctuation the value of H_{eff} should also predictably steadily rise with increase in the temperature of decomposition, as was observed experimentally. Increasing the decomposition temperature should also lower the degree of order in the Fe–Co phase. However, the reduced degree of order which is anticipated for equilibrium at higher temperatures will be affected by the altered changes in composition fluctuations and rate limitations thereby producing a degree of order which reaches a maximum at some temperatures below the order–disorder critical temperature, such as was found by Vintaykin *et al.* [6] for a decomposition temperature of 550° C.

In Fe–Co alloys with cobalt contents exceeding 30%, increase in order causes an increase in the value of the first anisotropy constant K_1 [40], and thereby the intrinsic coercivity and remanence are also increased. Thus a peak in these parameters could be anticipated at the temperature which maximises the degree of order in the alloy currently investigated; however, this peak might occur during isothermal decomposition or during the ageing which succeeds it. While the hyperfine field is also known to be order dependent the actual dependence is uncertain [28, 41]; the magnitude of the increase in H_{eff} (20 kOe) would also appear to be too large for order–disorder influence alone [41]. The degree of H_{eff} increase is also influenced by the particular composition of the Fe–Co rich phase; this is because the increase in K_1 obtained on ordering will be partly negated by the decrease in K_1 resulting from a rise in the Co content.

The weakly ferromagnetic state of the Cr-rich phase which is observable after the initial isothermal decomposition treatment suggests an explanation for the lack of evidence of any noticeable degree of induced anisotropy in the corresponding Mössbauer spectra. At the field decomposition temperatures involved, the Cr-rich phase will be paramagnetic since for chromium compositions exceeding 30% Cr the Curie temperature lies below 600° C [42]. In fact, after the initial isothermal treatment the hyperfine field values indicate a Cr composition of $\gtrsim$ 50%. During the later stages of decomposition much higher chromium contents are applicable. It is to be expected that a larger degree of induced (shape?) anisotropy in the Fe–Co regions has been effected during the application of the external magnetic field at the decomposition treatment temperature. However, on subsequent cooling to room temperature, i.e. under the conditions for the Mössbauer spectra determinations the Cr-rich phase is also ferromagnetic as evidenced by the resulting 6-line spectra. Because the anisotropy energy is dependent on the difference in saturation magnetization between the two phases, and as this difference is significantly reduced at temperatures below the Curie point for the α_2 phase, the measurable effects of the induced anisotropy will become correspondingly reduced at room temperature.

Acknowledgements

The authors wish to thank Mr P. Picone for valuable assistance during the Mössbauer experiments

and in the computer fitting of the experimental data, and Miss S. Aylward for the re-drawing of the spectra. The encouragement of Professor Yoji Nakamura of Kyoto University and of Professor Yoshiro Iwama of Nagoya University, whose help in making available important and unpublished background material is also acknowledged.

References

1. H. KANEKO, M. HOMMA and K. NAKAMURA, "Proceedings of the 17th Conference on Magnetism and Magnetic Materials", Chicago, 1971 (A.I.P., New York, 1971) p. 1088.
2. R. CREMER and I. PFEIFFER, *Physica* **80B** (1975). 164.
3. I. M. MAGAT, G. V. IVANOVA, T. P. LAPINA, L. V. SOLINA and YA. S. SHUR, *The Physics of Metals and Metallography* **40** (1975) 43.
4. Y. IWAMA, M. INAGAKI and Y. HOSHINO, Paper submitted to the 71st convention, Japan Institute of Metals, Autumn meeting, Nagoya University, 1972 (Proceedings unpublished).
5. M. INAGAKI, K. KIMURA and Y. IWAMA, Paper submitted to the 75th convention Japan Institute of Metals, Autumn meeting, Kinki University, 1974 (proceedings unpublished).
6. YE. Z. VINTAYKIN, G. G. URUSHADZE, I. S. BELYATSKAYA and YE. A. SUKHAROVA, *The Physics of Metals and Metallography* **38** (1974) 102.
7. T. SATOW, S. KACHI and K. IWASE, *Sci. Rep. Res. Inst. Tohoku University* 8 (1956) 502.
8. YE. Z. VINTAYKIN, *Dokl. Akad. Nauk SSSR* **118** (1958) 977.
9. V. V. OVCHINNIKOV, N. V. ZVIGINSTEV, V. S. LIVINOV and V. A. OSMINKIN, *Fiz. Metallov. e. Metalloved.* **42** (1976) 310.
10. H. KANEKO, M. HOMMA, M. OKADA, S. NAKAMURA and N. IKUTA, 21st Conference on Magnetism and Magnetic Materials, AIP Conference Proceedings No. 29 (1975) 620.
11. M. OKADA, M. HOMMA, N. KANEKO and G. THOMAS. 34th Annual Proceedings Electron Microscopy Society of America, Florida (1976) 686.
12. M. E. HOUGHTON and P. L. ROSSITER, To be published.
13. P. GRAY, D. HADFIELD and H. W. RAYSON, Proceedings 3rd European Conference on Hard Magnetic Materials, Amsterdam, 1974, p. 193.
14. M. McCAIG, *IEEE Trans Magnetics* **11** (1975) 1443.
15. H. KANEKO, M. HOMMA and T. MINOWA, *ibid* **12** (1976) 977.
16. H. KANEKO, M. HOMMA, K. NAKAMURA and M. MIRA, *ibid* 8 (1972) 347.
17. H. KANEKO, M. HOMMA, T. FUKUNAGA and M. OKADA, *ibid* **11** (1975) 1440.
18. A. HIGUCHI, M. KAMIYA and K. SUZUKI, Proceedings 3rd European Conference on Hard Magnetic Materials, Amsterdam, 1974, p. 201.
19. W. WRIGHT, R. E. JOHNSON and P. L. BURKINSHAW, *ibid* p. 197.
20. M. G. LUZHINSKAYA, N. F. SHILOVA and YA. S. SHUR, *Fiz. Metall. e Metalloved.* **40** (1975) 748.
21. SONG JIN TAE, *Journal Korean Inst. of Metals* **12** (1974) 250.
22. *Idem, ibid* **13** (1975) 267.
23. P. GRAY, H. W. RAYSON and D. HADFIELD, 2nd Conference on advances in magnetic materials and their applications, London, 1976 p. 153.
24. T. MIYAZAKI, M. NAKAGAKI and E. YAJIMA, *Journal Jap. Inst. Metals* 38 (1974) 70.
25. V. GONSER, "Topics in applied Physics", Vol. 5 (Springer-Verlag, Berlin, 1975).
26. R. TAHARA, Y. NAKAMURA, M. INAGAKI and Y. IWAMA, "Proceedings of the International Conference on Mössbauer Spectrocopy Cracow" Vol. 1 (1975) p. 107.
27. G. DEHE, B. SEIDEL and W. MEISEL, *Nuclear Inst. Methods* **133** (1976) 381.
28. C. E. JOHNSON, M. S. RIDOUT and T. E. CRANSHAW, *Proc. Phys. Soc.* **81** (1963) 1079.
29. S. J. CAMPBELL and P. E. CLARK, *J. Phys. F. Metal Phys.* 4 (1974) 1073.
30. R. B. ROY and B. SOLLY, *Scandinavian J. Metallurgy* **2** (1973) 243.
31. "Mössbauer Effect Data Index", edited by J. C. Stevens and V. E. Stevens (Plenum Press, New York, 1975) p.63.
32. S. ARAJS and G. R. DUNMYRE, *J. Appl. Phys.* **37** (1966) 1017.
33. A. G. KHACHATURIAN, *IEEE Trans on Magnetics* **6** (1970) 233.
34. I. PFEIFFER, *Cobalt* **44** (1969) 115.
35. Y. IWAMA and M. TAKEUCHI, *Trans. Japan Inst. Metals* **15** (1974) 371.
36. YE. G. POVOLOTSKIY, V. N. SOPLYACHENKO and G. G. BELOLIPTSEV, *Phys. Met. Metallog.* **39** (1976) 138.
37. N. D. TOMOSHOV, "Theory of Corrosion and Protection of Metals" (McMillan & Co., New York, 1966) p. 144.
38. M. POURBAIX, "Atlas of Electrochemical Equilibria in Aqueous Solutions" (Pergamon Press, Oxford, 1966) p. 70.
39. J. E. HILLIARD, "Phase Transformations" (A.S.M., Ohio, 1970) p. 497.
40. R. C. HALL, *J. Appl. Phys.* **31** (1960) 157S.
41. B. de MAYO P. W. FORESTER and S. SPOONER, *ibid* **41** (1970) 1319.
42. M. FALLOT, *Ann. Phys,* **6** (1936) 305.

Received 6 April and accepted 16 May 1977.